Optimal Temperature Modulation of MOS Gas Sensors by System Identification

Nimisha Dutta and Manabendra Bhuyan

Electronics and Communication Engineering, Tezpur University, India, Tezpur
nimisha.dutta0@gmail.com, manab@tezu.ernet.in

Abstract

Temperature modulation of metal oxide semiconductor (MOS) gas sensors has been widely used due to its higher discriminating power. The temperature modulation alters the kinetics of the gas-sensor interaction leading to characteristic response patterns. However, the selection of frequencies and duty cycles is based on trial and error method. In this paper, we have introduced a method to systematically determine the optimal set of modulation frequencies and duty cycles using system identification theory for sensor modeling. Pulse modulation being a popular method of feature extraction of MOS sensors, optimization of parameters of pulse modulation becomes very significant. In our work, system identification has been applied to select the sensor model that provides the most stable and desired sensor response, hence solving problem of choosing the best frequency and duty cycle of the temperature modulating signal of the MOS sensor. The estimation of model parameters is done using iterative prediction-error minimization (PEM) method. The best suited transfer function was chosen for the MOS gas sensors based on the sensor stability and then the sensors were operated at the respective best frequencies and duty cycles. Principal Component Analysis (PCA) was used to visualize the different sample gas patterns. Data classification was performed using supervised neural network classifiers; namely the Multi-Layer Perceptron (MLP) network and Radial Basis Function (RBF) network and the classification percentage before and after optimization were compared henceforth.

Keywords: *Temperature Modulation, System Identification, Principal Component Analysis, Artificial Neural Network (ANN)*

1. Introduction

Metal oxide semiconductor (MOS) based gas sensors have been widely used in gas detection. Their advantages include low cost and high sensitivity along with disadvantages such as lack of stability and selectivity. Although MOS sensors show such advantages, they exhibit a series of unpleasant characteristics such as cross-sensitivity, drift, ageing, poisoning etc. They are poorly selective and are prone to response drift. In practical applications, various methods are usually used to overcome such drawbacks, for example, using chromatographic columns to separate components, by operating at different temperatures [1]-[4], by choosing different burning- in procedures, dopants, surface chemical modification [5]-[7] etc. Among the different approaches envisaged to overcome these drawbacks, modulating the temperature of gas sensors have been remarkably successful in many applications [8]-[11].

2. Temperature Modulation and System Identification in Gas Sensors

2.1. Temperature Modulation

One of the most established ways of improving the selectivity of MOS sensors is by periodically varying the sensors' operating temperature. Researchers have reported on the advantage of temperature modulation on a ceramic metal oxide sensor at two different temperatures to detect the presence of carbon mono-oxide [12]-[14]. Work has been carried on the temperature modulation using square wave to quantify hydrogen sulphide [15, 16]. To discriminate between different gases, modulating patterns such as sawtooth, triangular and square were also applied to the sensors [17]. The sinusoidal variation in the temperature also enhanced the classification of different gases. A number of works on the cyclic variations of the sensor heater voltage have been reported by many authors [8] and [18]. The response of the gas sensors to modulating temperature primarily depends on the analytical model which is based on the physical and chemical properties of the sensor material. By choosing the best function and the best frequency to achieve a stable dynamics that follow the concentration of the analyte will be an important optimization strategy of the gas sensor.

The frequency of modulation is selected on trial and error method in many of the works based on temperature modulation. One of the successful methods of selecting optimized frequency was based on system identification through multilevel pseudorandom sequences [19] and pseudorandom binary sequences [20]. Since pulse modulation is a popular method of feature extraction of MOS sensors, optimization of parameters of pulse modulation will be a remarkable strategy in this area. To overcome the problem of choosing the best frequency of the temperature modulating signal of the MOS sensor, system identification has been applied to select the sensor model that provides the most stable and desired sensor response. We have chosen a set of optimized frequencies for the first time in MOS sensors using system identification theory for sensor modeling.

2.2. System Identification in MOS Sensors

System identification deals with building of mathematical models of dynamical systems based on the observed data from the system. To build mathematical models of dynamical systems from measured data, system identification techniques has been employed which includes the optimal design of experiments for efficiently generating informative data for fitting such models. This data-driven approach helps to observe the gas sensor as a dynamic system and employ suitable methods so that its behavior at different conditions can be modeled. We can interpret from the physical phenomenon of the sensor that the MOS sensor models rely on the mechanism of adsorption of gas molecules by the sensor film, at an elevated temperature and then the change in the electrical conductance of the sensor material. The above stages, though looks distinct, physically it is difficult to distinctly segregate the whole model into such distinct stages.

The work focuses on the optimized temperature modulation based on the system identification technique. The best suited transfer function was chosen for the MOS gas sensors based on the sensor stability and then the sensors were operated at the respective best frequencies and duty cycles, the classification of various gases were performed using the Artificial Neural Network (ANN).

3. State-Space Models

The system identification technique helps in model analysis and transformation, such as reducing model order and converting between discrete-time and continuous-time representations and also simulation or prediction of future output using the model. In our study the estimated model is a Linear Time Invariant (LTI) model in which the following model conversions are implemented:

i. Continuous time.

ii. Discrete time

iii. State-space

iv. Transfer function

v. Zero-pole gain

The estimation of model parameters is done using iterative prediction-error minimization (PEM) method. This method is the basic estimation procedure that supports both time domain and frequency domain signals. If the data is continuous time (frequency-domain) data, a corresponding continuous time state-space model is estimated.

In a continuous linear time invariant (LTI) system, the state-space model representation is:

$$\dot{x}(t) = Ax(t) + Bu(t) \tag{1}$$

$$y(t) = Cx(t) + Du(t) \tag{2}$$

where the vectors *x(t)*, *y(t)* and *u(t)* are state vector, output vector and input vector respectively. The matrices *A*, *B*, *C* and *D* are state matrix, input matrix, output matrix and feedforward matrix respectively of proper dimensions. Since the system identification has been performed from the discrete data of input-output, the discrete state space model is more relevant than continuous time model. The discrete state-space model is given by:

$$x(KT + T) = Ax(KT) + Bu(KT) \tag{3}$$

$$Y(KT) = Cx(KT) + Du(KT) \tag{4}$$

where *K* is the sampling instant and *T* is the sampling interval. The LTI system can be represented in continuous time transfer function as-

$$y(t) = Hu(t) \tag{5}$$

where the transfer function *H* in Laplace domain can be represented using state-matrices as-

$$\hat{H}(s) = C(sI - A)^{-1} B + D \tag{6}$$

and it can be reduced to a form,

$$\hat{H}(s) = \frac{b_0 s^m + b_0 s^{m-1} + ... + b_m}{s^n + a_1 s^{n-1} + ... + a_n} \tag{7}$$

Further the z-transform of the LTI model can be represented as-

$$\hat{H}(z) = \frac{b_0 z^m + b_0 z^{m-1} + ... + b_m}{z^n + a_1 z^{n-1} + ... + a_n} \tag{8}$$

The dynamic measurement, when the sensor temperature is modulated, the complicated response transients are considered to be related to different reaction kinetics of the gas molecules. At low temperatures mainly surface reactions occur while at high temperatures bulk reactions between point defects in the semiconductor lattice and gaseous oxygen molecules occur. In both cases, the adsorption at active sites occurs first followed by some catalytic reactions. The oxygen adsorbates are partly consumed by oxidation of target gases on the semiconductor surface during the static measurement. The amount of chemisorbed oxygen decreases and hence the conductance increases. Therefore the resistance change of MOS sensors shows that the concentration of chemisorbed oxygen changes at the grain boundary. In the adsorption process the conductance increases with decrease in the concentration of chemisorbed oxygen.

The frequency and duty cycle of the pulse temperature signal significantly influences the dynamics of the sensor. This is because, the time for the reaction kinetics should match to the time for the sensor heating process. In this work the sensor model equations has been derived for the pulse frequencies of 10mHz, 40mHz, 80mHz and 120mHz and duty cycles of 50% and 75% i.e. eight different sensor models for each of the sensors have been identified. The stability of the models has been verified by calculating the overshoot percentage and from the pole-zero plots. This analysis gives an interesting result that the sensor models can be chosen with the best dynamic performance based on stability analysis and accordingly the corresponding best frequency and duty cycle has been determined. We are able to derive the various transfer functions under stable and unstable modes by PEM technique in MATLAB.

4. Sensor Data Classification

In many works [21]-[23], the authors described techniques for extracting and using the steady-state, the slope as well as the transient response information from the sensor's response. The classification of gas species has been carried out based on the features that depend on the reaction time and recovery time [24, 25].

The classification involves the following steps namely: feature extraction and pre-processing of the sensor response, principal component analysis (PCA) and then classification using ANN. The traditional method for feature extraction is Principal Component Analysis (PCA). This was done to reduce the dimensionality of the measurement space, and to extract relevant information for 'pattern recognition'. Moreover, optimum feature extraction helps in removing a major portion of redundant data, which may be perceived as noise in the signal. The resulting low-dimensional feature vector was then used for the classification of the data. PCA is used for data visualization. It is useful for visualizing any patterns existing in the response of a multisensory array data.

Pattern recognition techniques based on artificial neural networks (ANN) approaches were very widely used for gas sensors [26]. Two different NN structures namely MLP and RBF were adopted for this stage of data classification. The MLP learns by supervision, during the training phase it is presented with training vectors together with the associated targets corresponding to the specific tea aromas. It learns from the input data by adjusting the weights in the network using its specific learning algorithm; many different training algorithms exist that can be applied to the MLP. The purpose of this algorithm is to minimise the difference between the generated network output and the desired output; termed the error. The RBF network has been shown to be an efficient approach for interpolating scattered data and has been applied in various fields. It has a similar architecture to the MLP, exhibiting fully inter-connected layers. The MLP learns by supervision and the purpose of this algorithm is to minimise the difference between the generated network output and the desired output;

termed the error. The RBF network has been shown to be an efficient approach for interpolating scattered data and has been applied in various fields [27].

The work focuses on the achieving of better classification percentage of the sample gases with the optimized temperature modulation. The time constant of the sensor response has also been used as a feature of ANN classifier in [28]. In this work also the classification has been performed by using time constant of response curve of the dynamic classification.

5. Experiment

Two MOS gas sensors (TGS-2611 and TGS-842 of Figaro, Japan) was conducted for different pulse modulating temperature in the presence of input odor. Figure 1 shows the experimental set-up. The heater voltage modulation patterns (frequency and duty cycle) of the sensors were controlled by a PC through a Data Acquisition card (PCI6024E, National Instruments) and LabVIEW. Analog output of the card was applied to the gate of a MOSFET which supplies the modulating voltage to the sensors. Therefore, the heater voltage +VH accordingly followed the pulse signal to excite the sensor. The sensor output was interfaced to the PC through the DAQ card. The sample gas and the clean air flow were directed into the sensor head block by two diaphragm pumps through teflon pipes. The pumps were controlled by the PC through a driver circuit consisting of relays and transistor switches. The sequence of 'purging' and 'refreshing' with proper time duration was controlled through the DAQ card by the PC using LabVIEW programming. The sensors were kept inside a chamber away from interfering gas so that the baseline is established with clean air. Before each run of data acquisition, the baseline was verified and when found deviated, it was corrected by applying clean air. It was found in each run of experiment that on application of clean air the sensor baseline settles to a fixed level ensuring absence of any interfering gas.

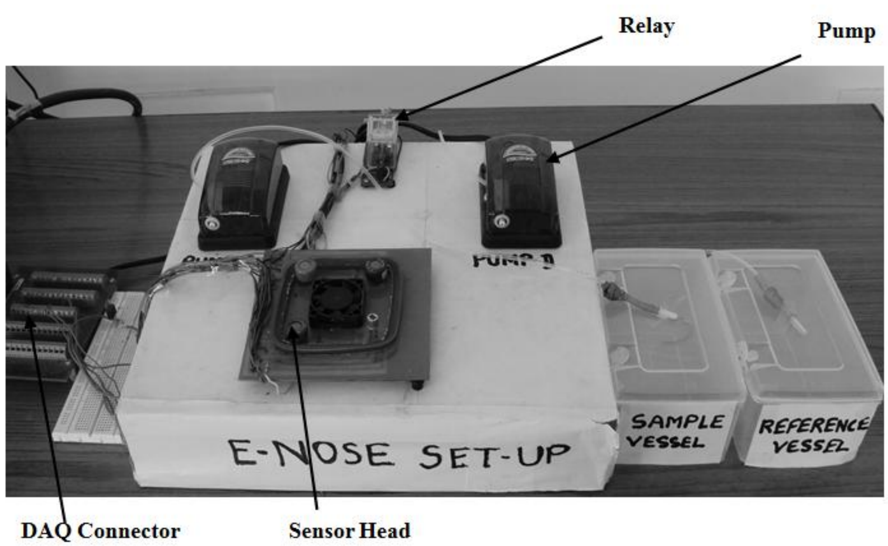

Figure 1. The Photograph of the Sensor Set-up

The experiment was conducted on the MOS sensors (TGS-2611 and TGS-842) with the application of ten different gas samples namely acetone, acetonitrile, chloroform, ethanol, ethyl acetate, isopropylalcohol, kerosene, methanol, n-hexane and petroleumether. During the application of gas, 100 complete pulse cycles were completed for each sample gas. At first, the sensor temperature was pulsed at a frequency of 10mHz and duty cycle of 50% to generate the sensor responses in the presence of the gas. This frequency was selected based in a trial and error procedure. The sensor signals were acquired at a sampling frequency of 1 kHz. The time constants were determined for each cycle and these time responses were used as the sample vectors for the gas classification. The sensor temperature was then pulsed at the selected frequency and duty cycle determined from system identification and the classification of gas was performed.

6. Results and Discussions

The input signal is the square pulse and the output is the sensor response as shown in Fig. 2 for sensor TGS-822. The input-output signal data obtained from the sensor response are then quantified by the system identification process. The model is estimated by the system identification technique and the stable transfer function is determined based on the best fit, pole zero plot and the overshoot percentage. Applying the respective best frequencies and duty cycles to the sensors the classification of different samples were done and the classification percentage before and after the optimal frequency modulation was found.

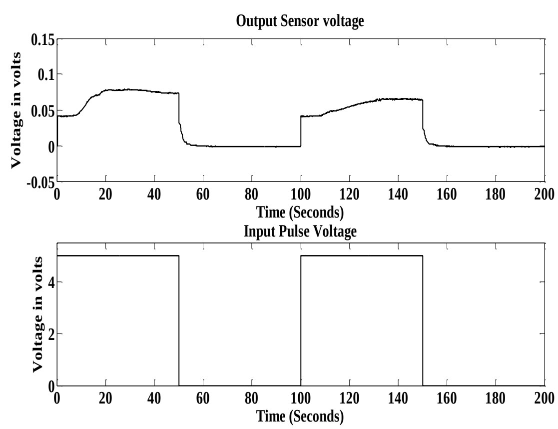

Figure 2. The Input-output Response of the Sensor TGS-842

The system identification is employed to determine the transfer function from the input pulse voltage. To ensure, how accurate the estimated transfer function is, a comparison is made between the simulated and the measured sensor output response. The model is selected for the smallest difference in between the actual response and the simulated response. This approach is termed as prediction error method. Figure 3 shows the comparison between the simulated and the measured results of the MOS sensors. The system identification gives us a transfer function of the sensor model in z-domain with a higher order approximation, however the model can be reduced to a lower order approximation say to order 2 or 1. Based on the best fit, the pole-zero plot and the overshoot percentage, the best transfer function is selected. Figure 4 shows the pole-zero diagrams of the transfer function and Fig.5 with zoomed visualization. As can be seen all the poles lie strictly inside the unit circle. The distance of the poles from the unit circle is calculated from the transfer function and is tabulated in Table 1. Another criterion for choosing the stable transfer function is the overshoot percentage calculated from the step response of the sensors as shown in Figure 6.

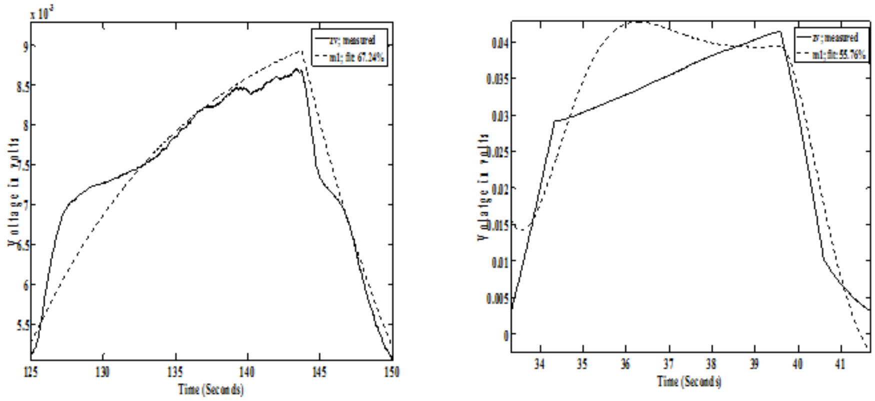

3(a) 3(b)

Figure 3. Sensor Responses Measured and Simulated for (a) TGS-2611 at 40mHz and 75% Duty Cycle and (b) TGS-842 at 120mHz and 75% Duty Cycle

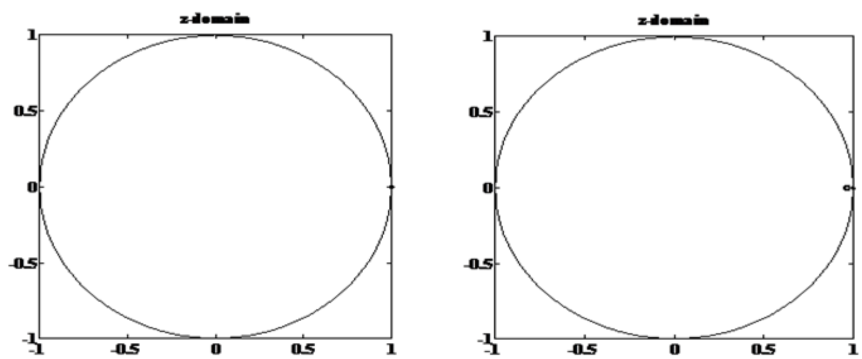

4(a) 4(b)

Figure 4. Pole-zero Plot of Transfer Function of Sensor (a) TGS-2611 in z-Domain 40mHz and 75% Duty Cycle and (b) TGS-842 in z-domain at 120mHz and 75% Duty Cycle

As shown in the table, the optimal frequency and duty cycle obtained for the sensors were 40mHz and 75% duty cycle and 120mHz and 75% duty cycle respectively. The data obtained from the sensors for the 10 sample gases before optimization were analyzed by Principal Component Analysis (PCA) and Artificial Neural Network (ANN) using MATLAB. The results of the PCA before the optimization of modulation are shown in Figure 7.

Table 1. Transfer Function Model Parameters of Three Sensors for Different Frequencies and Duty Cycles (The stable model parameters are shown in bold)

Sensors	Frequency (mHz)	Duty Cycle (%)	%age of best fit (%)	%age of overshoot (%)	Position of pole from center	Best transfer function
1	10	50	29.51	1.02	0.999	$H(z)_{40mHz} = \frac{(1.7\times10^{-7})}{(z-0.996)}$
	40		57.25	1.026	0.999	
	80		59.75	1.007	0.999	
	120		23.8	3.97	1	
	10	**75**	28.79	1.126	1	
	40		**67.24**	**0.96**	**0.996**	
	80		55.5	1.1	0.999	
	120		39.71	6.27	0.999	
2	10	50	1.01	1.22	1,1	$H(z)_{120mHz} = \frac{(4.248\times10^{-7})(z-0.9639)}{(z-0.9995)(z-0.9994)}$
	40		4.4	3.9	1.001,1	
	80		7.926	1.25	1.005,0.9995	
	120		55.76	1.02	0.9995,0.996	
	10	**75**	1.04	4.8	1.002,1.006	
	40		16	1.38	1.005,1.0006	
	80		40.06	1.035	0.9995,0.997	
	120		**63.43**	**1.015**	**0.9992,0.995**	

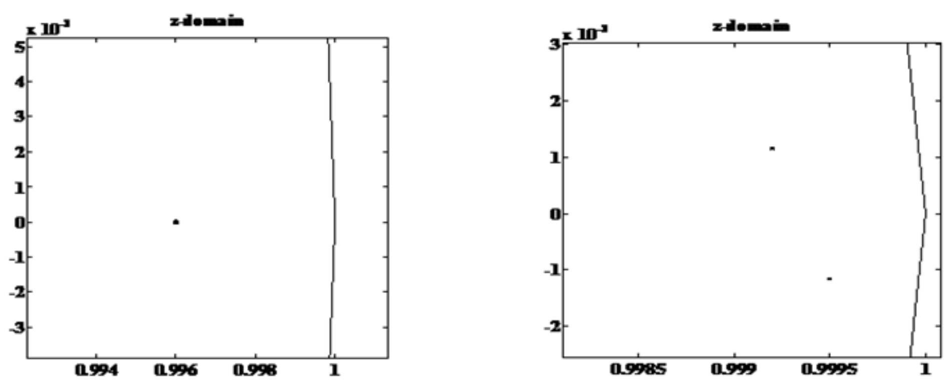

5(a) 5(b)

Figure 5. Zoomed part of the pole-zero plot of transfer function of sensor (a) TGS-2611 in z-domain at 40mHz and 75% duty cycle and (b) TGS-842 in z-domain at 120mHz and 75% duty cycle

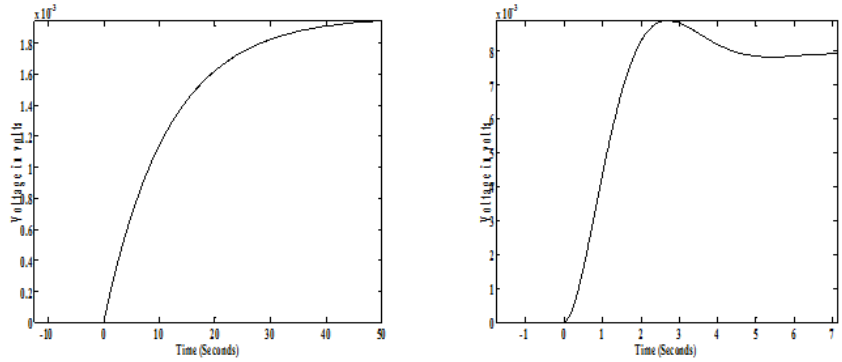

6(a) 6(b)

Figure 6. Step response of sensor (a) TGS-822 at 40mHz and 75% duty cycle and (b) TGS-822 at 40mHz and 75% duty cycle

The classification of data was performed using neural networks. MLP and RBF were used for the classification purpose. It was observed that training with MLP resulted in 74.6% classification accuracy whereas the RBF was able to classify the test sample with 87% accuracy. The system identification determined the most stable transfer function based on the best fit, the overshoot percentage and the pole-zero plot of the transfer function. Hence, by applying the three sensors at the respective best frequencies and duty cycle, the data was acquired for the 10 sample gases and the classification was done using ANN. The results of the PCA after the optimization of modulation are shown in Fig. 8. It was observed that training with MLP resulted in 86.7% classification accuracy whereas the RBF was able to classify the test sample with 93.4% accuracy. Table 2. shows the comparison of the classification percentage before and after the optimal modulation frequency determination.

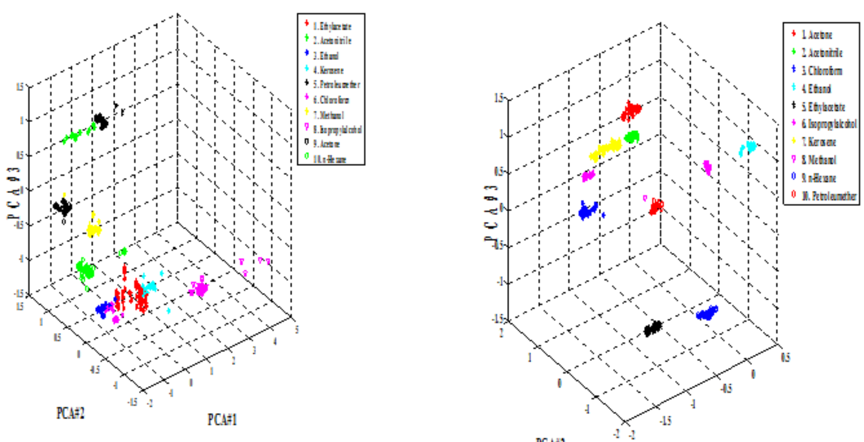

7(a) 7(b)

Figure 7(a). PCA before the optimization of modulation frequencies and (b) PCA after the optimization of modulation frequencies

Table 2. Comparison of the Classification Percentage

Classification mode	ANN Classifier	
	MLP	RBF
Before optimization of frequency and duty cycle	74.6%	87%
After optimization of frequency and duty cycle	86.7%	93.4%

7. Conclusions

Recent studies showed that selectivity could be enhanced by modulating the sensors' operating temperature. However, the selection of the frequencies used to modulate the sensors' temperature for a given gas-analysis application remained a non-systematic process based on the trial and error procedure.

In this paper, we have introduced a method to systematically determine the optimal set of modulation frequencies to solve a given gas-analysis application. The method is applied to MOS based gas sensors and the transfer function based on the best fit, pole-zero plot and the overshoot percentage was determined. The frequencies and duty cycles at which the transfer function was most stable for TGS-2611 and TGS-842 was determined as 40mHz and 75% and 120mHz and 75% respectively. These optimal set of modulation frequencies and duty cycles were then used for the gas-analysis. It is seen that the system identification technique could effectively find the modulation frequencies to obtain good results in the identification of the gases studied. The optimization ensured the classification of the gases upto 93.7%.

References

[1] A. P. Lee and B. J. Reedy, J. Sens. Actuators B, vol. 60, **(1999)**, pp. 35-42.
[2] A.Heiling, N. Barsan, U. Weimar, M. Schweizer-Berberich, J.W. Gardner and W. Gopel, J. Sens. Actuators B, vol. 43, **(1997)**, pp. 45-51.
[3] X. Huang, F. Meng, Z. Pi , W. Xu and J. Liu, J. Sens. Actuators B, vol. 99, **(2004)**, pp. 444–450.
[4] A. Vergara, E. Llobet, J. Brezmes, X. Vilanova, M. Stankova, I. Gracia, C. Cane and X. Correig, J. IEEE Sensors, **(2004)**.
[5] N. Barsan, R. Ionescu and A. Vancu, J. Sens. Actuators B, vol. 18–19, **(1994)**, pp. 466–469.
[6] U. Weimar and W. Gopel, J. Sens. Actuators B, vol. 26, **(1995)**, pp. 13.
[7] K. Wada and M. Egashira, J. Sens. Actuators B, vol. 53, **(1998)**, pp. 147–154.
[8] W. M. Sears, K. Colbow and F. Consadori, J. Semicond. Sci. Technol., vol. 4, **(1989)**, pp. 351– 359.
[9] W. M. Sears, K. Colbow and F. Consadori, J. Sens. Actuators, vol. 19, **(1989)**, pp. 333–349.
[10] S. Nakata, Y. Kaneda, H. Nakamura and K. Yoshikawa, Chem. Lett., **(1991)**, pp. 1505–1508.
[11] S. Nakata, H. Nakamura, K. Yoshikawa, J. Sens. Actuators B, vol. 8, **(1992)**, pp. 187–189.
[12] H. D. Le Vine, "Method and apparatus for operating a gas sensor", U.S. Patent 3906473, **(1975)** September 16.
[13] H. Eicker, "Method and apparatus for determining the concentration of one gaseous component in a mixture of gases", U.S. Patent 4012692, **(1977)** March 15.
[14] L. J. Owen, "Gas monitors", U.S. Patent 4185491, **(1980)** January 29.
[15] G. N. Advani, R. Beard and L. Nanis, "Gas measurement method", U.S. Patent 4399684, **(1983)** August 23.
[16] V. Lantto and P. Romppainen, "Response of some SnO2 gas sensors to H2S after quick cooling", J. Electrochem. Soc., vol. 135, **(1988)**, pp. 2550-2556.
[17] S. Bulkowiecki, G. Pfister, A. Reis, A. P. Troup and H. P. Ulli, "Gas or vapor alarm system including scanning gas sensors", U.S. Patent 4567475, **(1986)** January 28.
[18] W. M. Sears, K. Colbow and Franco Consadori, J. Sens. Actuators B, vol. 19, **(1989)**, pp. 333-349.

[19] A. Vergara, E. Llobet, J. Brezmes, P. Ivanova, X. Vilanova , I. Gracia , C. Can´e and X. Correig, J. Sens. Actuators B, vol. 111–112, **(2005)**, pp. 271–280.
[20] A. Vergara, E. Llobet, J. Brezmes, X. Vilanova ,P. Ivanova, I. Gracia , C. Can´e and X. Correig, J. IEEE Sensors,vol. 5, no. 6, **(2005)**.
[21] F. Sarry and M. Lumbreras, IEEE Trans. on Instrumentation and Measurement , vol. 49, no. 4, **(2000)**, pp. 809 – 812.
[22] E. Llobet, J. Brezmes, X. Vilanova, L. Fondevila and X. Correig, Proceedings of the International Conference on Solid State Sensors and Actuators, vol. 2, **(1997)**, pp. 971. Transducers '97, Chicago.
[23] H. Nanto, S. Tsubakino, M. Ikeda and F. Endo, J. Sens. Actuators B, vol. 25, no. 1–3, **(1995)**, pp. 794.
[24] S. Zhang, C. Xie, D. Zeng, H. Li, Z. Bai and S. Cai, J. IEEE Sensors, vol. 8, no.11, **(2008)**.
[25] S. Zhang, X. Xia, C. Xie, S. Cai, H. Li and D. Zeng, J. IEEE Sensors, vol. 9, no.12, **(2009)**.
[26] A Bermak, S. B Belhouari, M Shi and D. Martinez, Encyclopedia of Sensors, **(2006)**, pp. 1–17.
[27] J. Moody and C. Darken, **(1989)**, pp. 281–294.
[28] N. Dutta and M. Bhuyan, Proceedings of the Second International Conference on Emerging Applications of Information Technology, IEEE, **(2011)**, Kolkata, pp-231-234.